Journal of Materials Chemistry C

PAPER

View Article Online
View Journal | View Issue

Cite this: J. Mater. Chem. C, 2018, 6, 8999

New red-emitting Schiff base chelates: promising dyes for sensing and imaging of temperature and oxygen *via* phosphorescence decay time†

Sergey M. Borisov,*[a] Reinhold Pommer,[a] Jan Svec,[b] Sven Peters,[c] Veronika Novakova[b] and Ingo Klimant[a]

New complexes of Zn(II), Pd(II) and Pt(II) with Schiff bases are prepared in a one-step condensation of 4-(dibutylamino)-2-hydroxybenzaldehyde and 4,5-diaminophthalonitrile in the presence of a metal salt. The complexes possess efficient absorption in the blue-green part of the spectrum with molar absorption coefficients up to 98 000 M^{-1} cm^{-1}. The Pt(II) complex shows very strong red phosphorescence in anoxic solutions at room temperature with a quantum yield of 65% in toluene which places it among the brightest emitters available for this spectral range. The phosphorescence of the Pd(II) complex under the same conditions is very weak (Φ < 1%) but is enhanced to Φ > 10% upon immobilization into polymers. Optical thermometers based on self-referenced lifetime read-out are prepared upon immobilization of the dyes into gas-blocking poly(vinylidene chloride-*co*-acrylonitrile). At 25 °C, the materials based on Pd(II) and Pt(II) complexes show sensitivities of −2.1 and −0.52%τ/K, respectively. Application of the sensors for imaging of temperature on surfaces (planar optode) and for monitoring of fast temperature fluctuations (fiber-optic microsensor) is demonstrated. Immobilized into a gas-permeable matrix, the Pt(II) complex also performs as a promising oxygen-sensing material. The new systems are also attractive for imaging of oxygen or temperature with the help of multi-photon microscopy, due to a good match with the biological optical window and much better brightness under two photon excitation compared to that of the conventional Pt(II) *meso*-tetra-(pentafluorophenyl)porphyrin.

Received 4th June 2018,
Accepted 30th July 2018

DOI: 10.1039/c8tc02726a

rsc.li/materials-c

1. Introduction

Recent years have seen a great interest in new dyes which show thermally activated delayed fluorescence (TADF)[1–4] or phosphorescence,[5–8] at room temperature primarily due to their high potential as emitters in OLEDs.[6,7,9–11] Phosphorescent dyes have also been applied in various materials for optical sensing[12,13] (for example of oxygen,[14,15] glucose,[16] pH[17] or temperature[18]) and for bioimaging.[19–21] They also act as efficient sensitizers in triplet–triplet annihilation (TTA) based upconversion systems.[22–24] For sensing and imaging applications high brightness (defined as the product of the molar absorption coefficient ε and the luminescence quantum yield Φ) is of primary importance.

Although numerous metal-free emitters have been reported lately[25–30] most phosphorescent dyes are still covered by metal complexes. Platinum(II) and palladium(II) complexes with porphyrins and their derivatives (porphyrin lactones,[31] ketones,[32] *etc.*) are very popular phosphorescent emitters.[6,12] They feature tuneable spectral properties and good luminescence brightness. Ruthenium(II) polypyridyl complexes[33] and platinum(II) and iridium(III) cyclometalated complexes[34] with numerous ligands show long-lived metal-to-ligand charge-transfer luminescence but possess a lower brightness due to moderate ε. Therefore, they are less attractive for sensing and light conversion applications, except for a few representatives.[35,36] The same is true for TADF emitters which often have very high Φ, but low to moderate ε in the visible part of the spectrum.[37] Schiff bases form phosphorescent chelates with platinum(II) and palladium(II),[38–41] but the luminescence brightness is moderate either due to low ε[38–40] or low Φ.[41,42] Nevertheless, they were shown to be promising for application in OLEDs,[38–40] optical sensing[41] and TTA upconversion[41,43] and other energy-related applications.[44]

Sensors utilizing luminescent materials offer many advantages compared to conventional analytical methods including minimal invasiveness, comparably low cost, suitability for

[a] Institute of Analytical Chemistry and Food Chemistry, Graz University of Technology, Stremayrgasse 9, 8010, Graz, Austria. E-mail: sergey.borisov@tugraz.at
[b] Department of Pharmaceutical Chemistry and Pharmaceutical Analysis, Faculty of Pharmacy in Hradec Kralove, Charles University, Akademika Heyrovskeho 1203, Hradec Kralove, Czech Republic
[c] Department of Ophthalmology, University Hospital Jena, Jena, Germany

† Electronic supplementary information (ESI) available: Details on photophysical properties and calibrations, NMR, IR and mass-spectra. See DOI: 10.1039/c8tc02726a

imaging of analyte distribution and possibility of multi-parameter sensing with a single material. Temperature is undoubtedly one of the most important parameters which, among other methods, can be measured *via* change in the luminescent properties of an indicator,[18,45] in most cases either a (metal)-organic dye or an inorganic phosphor. Materials which utilize change of the comparably long luminescence lifetimes (μs–ms) are particularly attractive due to the self-reference character of the measurement and inexpensive equipment needed for the sensor read-out. Unfortunately, among numerous materials published[18] only a few are suitable for this read-out.

In this contribution we report new metal complexes of Schiff bases which can be conveniently accessed in a one-step procedure. We will show that the phosphorescent properties of the dyes enable their application as advanced molecular thermometers with lifetime-based read-out.

2. Experimental section

2.1 Materials

Zinc acetate dihydrate and palladium acetate were obtained from Aldrich, and methanesulfonic acid was obtained from ABCR. Polystyrene (PS; MW = 260 000 Da) was purchased from Acros Organics and poly(vinylidene chloride-*co*-acrylonitrile) (PViCl-PAN, 20 wt% acrylonitrile content, MW = 125 000 Da) was obtained from Scientific Polymer (www.scientificpolymer.com). Eudragit RL-100 copolymer (poly(ethylacrylate-*co*-methylmethacrylate-*co*-trimethyl-aminoethyl methacrylate), 8.85–11.96 wt% trimethyl-aminoethyl methacrylate units on a dry substance), MW = 150 000 Da, was obtained from Degussa (www.evonik.com). *N*,*N*-Bis(2,6-diisopropylphenyl)-1,6,7,12-tetraphenoxyperylene-3,4:9,10-tetracarboxylic acid bisimide (Lumogen Red) was obtained from Kremer Pigmente GmbH and Co. KG (Germany). Poly(ethylene terephthalate) (PET) support Melinex 505 was purchased from Pütz (Germany). Platinum(II) *meso*-(pentafluorophenyl)porphyrin (Pt-TFPP) was acquired from Frontier Scientific (Logan, UT, USA). Solvents were obtained from VWR and both were used as received. Nitrogen, argon and oxygen (both 99.999% purity) were purchased from Air Liquide (Austria) and Linde Gas (Austria), respectively.

Platinum(II) bis(benzonitrile)dichloride ($Pt(BN)_2Cl_2$) and 4-(dibutylamino)-2-hydroxybenzaldehyde were prepared according to the literature procedures.[41] The preparation of 4,5-diaminophthalonitrile is described elsewhere.[46,47]

Synthesis

*Zn(II) complex of (4E,5E)-4,5-bis(4-(dibutylamino)-2-hydroxybenzylideneamino)benzene-1,2-dinitrile (**Zn-1**).* 4-(Dibutylamino)-2-hydroxybenzaldehyde (196 mg, 0.79 mmol, 4.1 eq.) and 4,5-diaminophthalonitrile (30 mg, 0.19 mmol, 1 eq.) were dissolved in 8 mL of methanol and zinc acetate dihydrate (62 mg, 0.28 mmol, 1.5 eq.) was added. The suspension was ultrasonicated and transferred under nitrogen counterflow into a Schlenk flask. Methanesulfonic acid (10 μL, 15 mg, 0.15 mmol, 0.8 eq.) was added under vigorous stirring. The obtained solution was stirred at 40 °C resulting in the formation of a red sediment. After 120 minutes, the dispersion was cooled down to room temperature and the sediment isolated *via* centrifugation. The product was washed several times with methanol and cyclohexane to remove the excess of 4-(dibutylamino)-2-hydroxybenzaldehyde and dried in a drying cabinet. Yield: 75 mg (0.110 mmol, 58%).

^{1}H-NMR: (300 MHz, DMSO-d_6): δ [ppm] = 8.77 (s, 2H), 8.36 (s, 2H), 7.13 (m, 2H), 6.19 (d, 2H), 5.78 (s, 2H), 3.40 (m, 8H), 1.50 (m, 8H), 1.34 (m, 8H), 0.92 (m, 12H).

IR, (cm^{-1}): 2958, 2927, 2858, 2219, 1597, 1556, 1515, 1487, 1432, 1355, 1283, 1252, 1213, 1181, 1140, 1071, 1020, 920, 871, 820, 773, 732, 660, 598, 534.

HR MS (MALFDI-TOF) [*m*/*z*]: calc.: 682.2974, found: 682.3397.

*Pt(II) complex of (4E,5E)-4,5-bis(4-(dibutylamino)-2-hydroxybenzylideneamino)benzene-1,2-dinitrile (**Pt-1**).* 4-(Dibutylamino)-2-hydroxybenzaldehyde (321 mg, 1.29 mmol, 4.0 eq.) and 4,5-diaminophralonitrile (50.3 mg, 0.32 mmol, 1 eq.) were dissolved in a 15 mL ethanol : methanol mixture (2 : 1 v/v) and $Pt(BN)_2Cl_2$ (229 mg, 0.49 mmol, 1.5 eq.) was added. The yellow suspension was ultrasonicated and transferred under nitrogen counterflow into a round bottom flask. Methanesulfonic acid (15 μL, 22.2 mg, 0.23 mmol, 0.7 eq.) was added. The resulting red solution was stirred overnight at 60 °C.

The product was purified *via* column chromatography on silica gel (dichloromethane/cyclohexane 9 : 1 v/v, then dichloromethane/ethyl acetate 19 : 1). Yield: 14.5 mg (5.6%) of dark red powder.

^{1}H-NMR: (300 MHz, $CDCl_3$): δ [ppm] = 7.58 (s, 2H), 7.53 (s, 2H), 6.90 (d, 2H), 6.25 (s, 2H), 6.15 (d, 2H), 3.31 (m, 8H), 1.67 (m, 8H), 1.40 (m, 8H), 0.95 (t, 12H).

^{13}C-NMR: (76 MHz, $CDCl_3$): δ [ppm] = 167.2, 154.8, 147.1, 144.5, 136.3, 118.8, 115.9, 114.0, 109.5, 107.1, 100.0, 51.1, 29.8, 20.4, 14.0.

IR, (cm^{-1}): 2956, 2930, 2870, 2226, 1614, 1553, 1515, 1483, 1412, 1353, 1289, 1253, 1214, 1189, 1144, 1110, 1071, 918, 822, 775, 753, 659, 578, 536.

HR MS (MALFDI-TOF) [*m*/*z*]: calc.: 813.3308, found: 813.3668.

*Pd(II) complex of (4E,5E)-4,5-bis(4-(dibutylamino)-2-hydroxybenzylideneamino)benzene-1,2-dinitrile (**Pd-1**).* **Pd-1** was prepared analogously to **Pt-1** but using palladium acetate (144 mg, 0.64 mmol, 2 eq.) instead of $Pt(BN)_2Cl_2$. Yield: 131 mg (55%) of red powder.

^{1}H-NMR: (300 MHz, $CDCl_3$): δ [ppm] = 7.77 (s, 2H), 7.73 (s, 2H), 7.02 (d, 2H), 6.32 (s, 2H), 6.22 (d, 2H), 3.33 (m, 8H), 1.67 (m, 8H), 1.39 (m, 8H), 0.97 (t, 12H).

^{13}C-NMR: (75 MHz, $CDCl_3$): δ [ppm] = 168.9, 155.5, 148.2, 146.4, 137.0, 119.3, 115.9, 113.6, 109.9, 106.9, 99.7, 51.1, 29.9, 20.3, 14.0.

IR, (cm^{-1}): 2956, 2923, 2862, 2220, 1610, 1544, 1512, 1477, 1410, 1344, 1293, 1250, 1213, 1179, 1140, 1112, 1067, 900, 820, 769, 728, 654, 577, 533.

HR MS (MALFDI-TOF) [*m*/*z*]: calc.: 724.2674, found: 724.3104.

Preparation of the planar optodes. Sensor films were prepared by coating the dye "cocktails" on a dust-free PET support

using a Gardner (Pompano Beach, United States) coating knife (thickness of the wet film 25 μm). The ''cocktails'' contained 0.075 wt% of the dye and 10 wt% of the polymer dissolved in the solvent (chloroform for polystyrene and tetrahydrofuran for PViCl-PAN). The PViCl-PAN layers were coated in a glove box to avoid humidity interference during solvent evaporation.

The **Pd-1**/PViCl-PAN layer was additionally coated by a light-scattering layer prepared by coating a ''cocktail'' containing 200 mg of liphophilic titanium dioxide (P170, Kemira, Finland), 500 mg of silicone E4 (Wacker, Germany) and 800 mg of hexane. This layer was allowed to cure under ambient conditions for 24 h and was covered by a black layer using a graphite spray from Conrad (Austria).

Preparation of the fiber-optic microsensor. A 430 μm optical fiber (Industrial Fiber Optics Inc.) was flat broken and the tip was melted to produce a hemispherical shape. In a glove box, the tip of the fiber was dip-coated with a ''cocktail'' containing **Pt-1** (0.1 wt%) and PViCl-PAN (10 wt%) dissolved in tetrahydrofuran. The tip of the fiber was submerged in a 7 wt% solution of Cytop in a perfluorinated solvent (Solvay, Japan) and dried in a drying cabinet at 65 °C overnight.

Preparation of nanoparticles for 2-P measurements. Nanoparticles were prepared according to the literature procedure.[48] Briefly, the dye (**Pt-1** or **PtTFPP**) and RL-100 were dissolved in a tetrahydrofuran : acetone mixture (1 : 1 v/v; 0.2 wt% of the polymer in the solvent mixture). The nanoparticles were formed by rapid addition of water under vigorous stirring followed by evaporation of the organic solvents under reduced pressure. The nanoparticles contained 1 wt% of dye with respect to the polymer.

2.2 Measurements

Compound characterization and photophysical studies. ^{1}H and ^{13}C NMR spectra were recorded on a 300 MHz spectrometer (Bruker AVANCE III). Data analysis was done with the MestraNova NMR software. High resolution mass spectra were recorded using a Micromass TofSpec 2E as a positive reflector on a Bruker Ultraflex Extreme MALDI-TOF/TOF spectrometer. The mass spectra were analyzed with the FlexAnalysis 3.0 software (Bruker Daltonics).

The absorption spectra were recorded on a CARY 50 UV-Vis spectrophotometer from Varian (Palo Alto, United States). Luminescence spectra were acquired on a FluoroLog 3 spectrofluorometer from Horiba Scientific equipped with a NIR-sensitive R2658 photomultiplier from Hamamatsu. Relative luminescence quantum yields were determined according to Crosby and Demas[49] using solutions of Lumogen red in chloroform (Φ = 0.96)[50] and platinum(II) octaethylporphyrin in toluene (Φ = 0.41)[51] as references. The quantum yield of **Zn-1** was estimated using fluorescein as a standard (Φ = 0.90).[49] The solutions of the complexes were deoxygenated in a screw-cap cuvette (Hellma; Müllheim, Germany) by bubbling argon through the solution for 10 minutes. Absolute luminescence quantum yields of the dyes embedded in polymers and nanoparticles were measured using a Quanta-ϕ integrating sphere from Horiba. Deep temperature measurements were performed on a FluoroLog 3 spectrofluorometer with a solution of dyes in a mixture of toluene and tetrahydrofuran (4 : 6 v/v) which forms frozen glass at 77 K.

Luminescence decays were acquired in a time domain on a FluoroLog 3 spectrofluorometer equipped with a DeltaHub module (Horiba Scientific) controlling a SpectraLED-390 (λ = 392 nm) and using DAS-6 Analysis software for data analysis. In order to acquire the temperature dependence of the luminescence spectra/decay time, a sensor foil was placed in a 1 cm glass cuvette filled with water with the temperature adjusted with a Peltier-element cuvette adaptor from Varian.

Photostability tests. To access the photostability of the dyes, their solutions in toluene (HPLC-grade) placed in a screw-cap cuvette (Hellma) were illuminated with a high-power LED (λ_{max} 465 nm, www.LED-TECH.de). The light of the LED-array was focused onto the glass cuvette using a lens from Edmund optics. The photon flux was 5600 μmol s^{-1} m^{-2} (144 mW cm^{-2}) as determined with a Li-250A light meter from LI-COR Biosciences (www.licor.com). For measurements at air saturation the cuvette was unsealed and shaken after each irradiation interval to ensure air saturation in the sample. For measurements under anoxic conditions the dye solution in the cuvette was bubbled through with argon for ten minutes prior to the experiment.

Two-photon luminescence spectra. Two photon emission and excitation spectra were acquired on an inverted multiphoton laser scanning microscope (Axio Observer Z.1 and LSM 710 NLO, Carl Zeiss, Jena, Germany) in combination with a femtosecond Ti:Sapphire laser (Chameleon Ultra, Coherent Inc., Santa Clara, CA, USA). The Ti:Sapphire laser has a pulse repetition rate of 80 MHz, a pulse duration of 140 fs and provides a tunable wavelength range from 690 to 1080 nm. The spectral QUASAR detector of the LSM710 in a quantum corrected mode (energy per wavelength) has been utilized to record all the spectra in the range of 418 to 728 nm with a channel width of 10 nm. A 63× oil immersion objective (Plan-Apochromat, NA = 1.4, Zeiss) was used. The dispersion of the nanoparticles (50 μg mL^{-1}) in PBS buffer (150 mM, pH 7.4) was deoxygenated enzymatically with the help of glucose and glucose oxidase. The experiments were performed at 25 °C with a laser power of 10 mW calibrated using a microscope slide power sensor (S170C, Thorlabs Inc., Newton, NJ, USA).

Characterization of the sensing materials. The oxygen sensing properties of **Pt-1** in polystyrene were studied using a gas-mixing device based on two mass-flow controllers (Voegtlin red-y smart series, www.voegtlin.com) and custom-built software was used to adjust the oxygen partial pressure for the calibration by mixing nitrogen and oxygen. The temperature of the calibration gases and the sensing foil positioned in the flow-cell was adjusted with a Julabo F12-ED refrigerated/heating circulator (www.julabo.com).

The fiber-optic temperature microsensor was read-out with a modified Firesting-mini phase fluorometer from PyroScience (www.pyro-science.com). The device was equipped with a 465 nm excitation LED, a Linos DT-cyan dichroic mirror and a Schott OG 590 long-pass filter used in combination with a Deep

Golden Amber plastic filter from Lee filters (www.leefilters.com). The modulation frequency of 12 kHz was used. The fiber-optic probe was rapidly transferred between two water-filled beakers kept at 40 °C and ~1 °C (ice water). The PT-100 resistance thermometer used for comparison studies was read-out with a Firesting oxygen meter from PyroScience.

Imaging of the temperature planar sensor was performed with a Sensicam time-gated CCD camera (PCO, Germany) with the general set-up reported elsewhere.[52] Excitation was performed with a high power 458 nm 10 W LED array (www.led-tech.de). The average decay time was calculated from the luminescence intensities measured in two time windows.[52]

3. Results and discussion

3.1 Synthesis

The complexes were synthesized in one step upon condensation of 4-(dibutylamino)-2-hydroxybenzaldehyde with 4,5-diaminophthalonitrile in the presence of a salt of the respective metal and under acidic conditions (Fig. 1). While Zn(II) and Pd(II) could be obtained in good yield (>50%) the yield of the corresponding Pt(II) complex is much lower (~5%). Our attempts to prepare the corresponding metal-free ligand *via* reaction of 4-(dibutylamino)-2-hydroxybenzaldehyde with 4,5-diaminophthalonitrile under acidic conditions failed since only a monosubstituted product was formed (ESI†). We also attempted to prepare chelates with other metal ions such as Gd(III) and Yb(III). Despite intriguing photophysical properties (see below) these derivatives could not be isolated due to poor stability and have an unknown stoichiometry.

The complexes of Pt(II) and Pd(II) show good solubility in organic solvents. In contrast, the Zn(II) complex is poorly soluble in non-coordinating solvents but dissolves fairly well in dimethylformamide. Addition of small amounts of coordinating pyridine strongly enhances the solubility of the Zn(II) complex in other solvents.

3.2 Photophysical properties

The absorption of the new complexes is shown in Fig. 2. As can be seen, the dyes efficiently absorb in the blue-green part of the electromagnetic spectrum. The absorption of the Pt(II) and

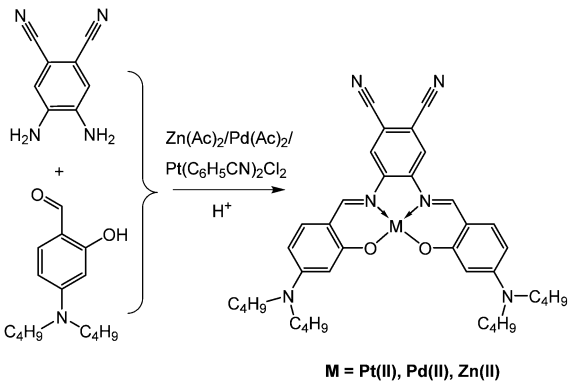

Fig. 1 Synthesis of the Schiff base complexes with **1**.

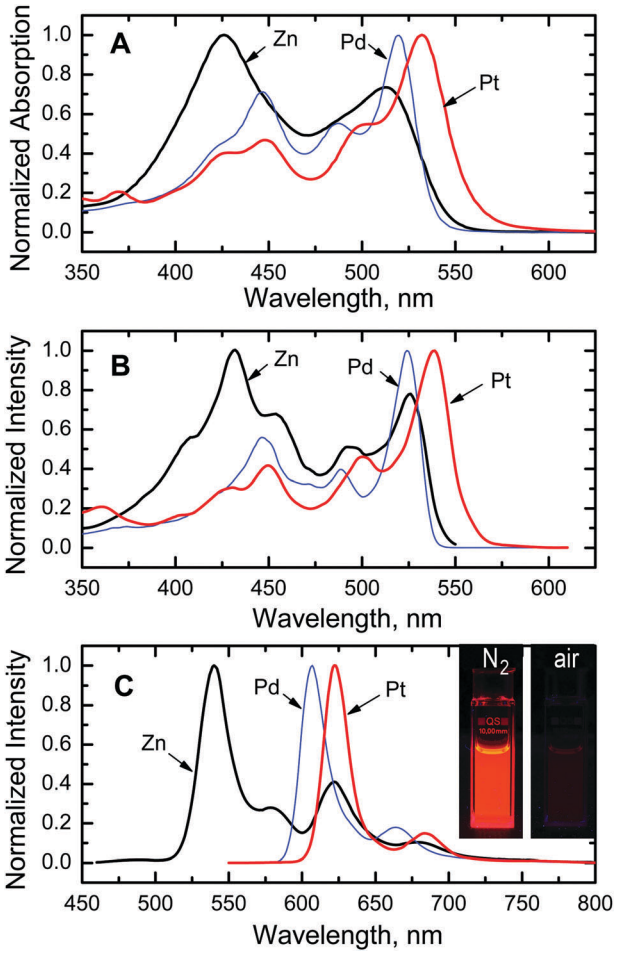

Fig. 2 Spectral properties of the Schiff base complexes with **1**. (A) Absorption spectra in toluene at room temperature; (B) excitation spectra in toluene : THF (4 : 6, v/v) at 77 K; (C) emission spectra in toluene : THF (4 : 6, v/v) at 77 K. The inset shows the emission of **Pt-1** in anoxic (left) and air-saturated (right) toluene at room temperature.

Pd(II) complexes is particularly efficient with the molar absorption coefficients ε exceeding 85 000 M^{-1} cm^{-1} (Table 1) which is explained by the donor–acceptor character of the chromophore. In fact, similar Pt(II) complexes of Schiff bases lacking the donor–acceptor character feature about 10-fold lower molar absorption coefficients in the visible part of the spectrum.[39] The ε values are also much higher than those for most reported Pt(II) and Pd(II) complexes with the exception of π-extended porphyrins. Interestingly, the absorption bands of the Pt(II) complex are ~12 nm bathochromically shifted compared to the Pd(II) dye. This trend is in good agreement with the effect observed for reported Schiff base complexes.[41]

Among the new dyes, the Pt(II) complex **Pt-1** was found to be highly emissive in anoxic solutions at room temperature (Fig. 2C, inset; Fig. S1, ESI,† Table 1). The emission is attributed to phosphorescence due to the decay time in the microsecond time domain (10.3 μs). The phosphorescence quantum yield is very high (65%) resulting in unmatched overall brightness of the compound. The brightness of the Pt(II) complex ($\varepsilon \cdot \Phi$ = 63 000) is comparable to that of the Ir(III) coumarin complexes

Table 1 Photophysical properties of the new complexes: maxima of the absorption and emission spectra (λ_{max} abs and λ_{max} em, respectively); molar absorption coefficients ε; luminescence quantum yields Φ for fluorescence (fl) and phosphorescence (phos); luminescence decay times τ

Complex	λ_{max} abs (ε), nm (M^{-1} cm^{-1})[a]	λ_{max} em, nm at 293 K[a]	Φ at 293 K[a]	τ, s at 293 K[a]	λ_{max} em, nm at 77 K[b]	Φ at 77 K[b]	τ, s at 77 K[b]
Zn-1[c]	426 (65 000); 513 (44 600)	554 (fl)	0.31 (fl), 0.03 (df)	n.d.	541 (fl); 579 (fl); 622 (phos), 683 (phos)	0.58 (fl), 0.15 (phos)	0.17 (phos)
Pd-1	447 (60 800); 487 (55 000); 520 (85 600)	613 (phos)	0.0006	n.d.	607	0.62	325×10^{-6}
Pt-1	448 (45 500); 499 (52 200); 532 (96 700)	627 (phos)	0.65	10.3×10^{-6}	622	0.61	12.7×10^{-6}

[a] In toluene. [b] In toluene : THF (4 : 6), v/v. [c] Small amount of pyridine added to increase the solubility.

($\varepsilon \cdot \Phi$ = 50 000 for $Ir(C_S)_2(acac)$)[35] which are among the brightest phosphorescent emitters reported so far. Notably, the absorption and emission bands of **Pt-1** are bathochromically shifted by ~60 nm compared to the Ir(III) complex (λ_{max} 472 and 563 nm for absorption and emission, respectively).[35] Thus, **Pt-1** covers a very important spectral range complementing the existing palette of bright phosphorescent emitters. The most intense band (λ_{max} 532 nm) shows excellent compatibility with the emission of bright green LEDs which is highly attractive for realization of compact devices for sensing applications.

In contrast to **Pt-1**, the Pd(II) complex **Pd-1** is only weakly emissive in solution at room temperature with the phosphorescence quantum yield well below 1%. Interestingly, at 77 K the phosphorescence of both complexes is similarly efficient (Fig. 2C and Table 1).

The Zn(II) complex **Zn-1**, shows bright green fluorescence in solution at room temperature (Fig. S2, ESI,† λ_{max} 554 nm, Φ = 31%). The absorption and emission spectra match very well with those obtained in the literature for a very similar complex of Zn(II) which bears ethyl groups instead of butyl groups.[53] The fluorescence intensity is enhanced upon deoxygenation, indicating the contribution of thermally-activated delayed fluorescence (TADF). In good agreement with this observation, in frozen glass at 77 K phosphorescence is observed instead of TADF (Fig. 2C). The phosphorescence decay time at 77 K is extremely long (0.17 s). Under the same conditions, the phosphorescence decay time of the Pd(II) and Pt(II) complexes is much shorter (325 and 12.7 μs, respectively) which is explained by the heavy atom effect in these complexes. Due to the ability of Zn(II) to coordinate additional ligands, investigation of complexes with pyridyl-functionalized ligands[54,55] may be an interesting direction for future work particularly in view of the potential applications of such dyes in light-emitting diodes.[54]

Encouraged by the excellent photophysical properties of the new Pt(II) complex we evaluated the ability of the new ligand to act as a sensitizer of the lanthanide luminescence. Although the complexes could not be isolated in a pure form and readily hydrolysed upon purification, the spectral properties in solution indicate the high potential of the new Schiff base to act as an efficient antenna. In fact, the Gd(III) chelate (stabilized in basic media in the presence of PF_6^- ions) showed efficient phosphorescence (λ_{max} = 618 nm, τ = 66 μs) in anoxic solutions at room temperature (Fig. S3, ESI†). When complexed with Yb(III), the Schiff base was able to sensitize the luminescence of this lanthanide with characteristic peaks at 974 and 1020 nm (Fig. S4, ESI†). Evidently, to make full use of the excellent sensitization properties of the new antenna, the stability of the complexes has to be enhanced, for instance by exploring the stabilization strategies reported in the literature (additional coordination sites in the Schiff base structure).[56,57]

High brightness of the Pt(II) complex suggests many potential applications, for instance as an advanced label for time-resolved measurement or as an oxygen probe. Suitability for multi-photon excitation is of particular interest since despite the large number of multi-photon emitters reported in the last few years[58,59] rather few analyte-sensitive probes suitable for this method have been reported. For example, several probes for two-photon (2-P) imaging of oxygen distribution have been reported by Vinogradov and co-workers[60–62] but a rather sophisticated design is important to achieve high multi-photon excitability. The new Pt(II) chelate may represent a simple alternative to these systems due to the push–pull character favouring 2-P absorption. Indeed, similar structures were demonstrated to possess significantly higher 2-P absorption cross-sections than conventional dyes.[53] In order to evaluate the potential of **Pt-1** for 2-P imaging the dye was embedded into polymeric nanoparticles. We used Rl-100 as a matrix since the nanoparticles prepared from this polymer were previously demonstrated to have high potential for intracellular imaging.[48] For comparison, we also stained the Rl-100 beads with platinum(II) tetra-pentafluorophenylporphyrin (**Pt-TFPP**) which is the most commonly used oxygen indicator. The emission spectrum of both dyes is very similar (Fig. 3A). The 2-P emission spectrum of **Pt-1** matches very well with the emission of the dye under 1-P excitation (Fig. S1, ESI†). As can be seen from Fig. 3B, the 2-P emission of **Pt-TFPP** is excitable at about 1000 nm. In contrast, the 2-P excitation spectrum of **Pt-1** is very broad and extends over the whole NIR part of the spectrum. Overall, the emission of the Schiff base under 2-P excitation is 10-fold stronger than that of **PtTFPP**. This difference is even higher if the Schiff base is excited at about 840 nm and not at 1050 nm. Estimation of phosphorescence quantum yields (anoxic conditions) for both dyes in Rl-100 nanoparticles revealed the values of 0.16 and 0.26 for **Pt-1** and **PtTFPP**, respectively. Thus, the Φ of **Pt-1** in Rl-100 beads is significantly lower than that in toluene

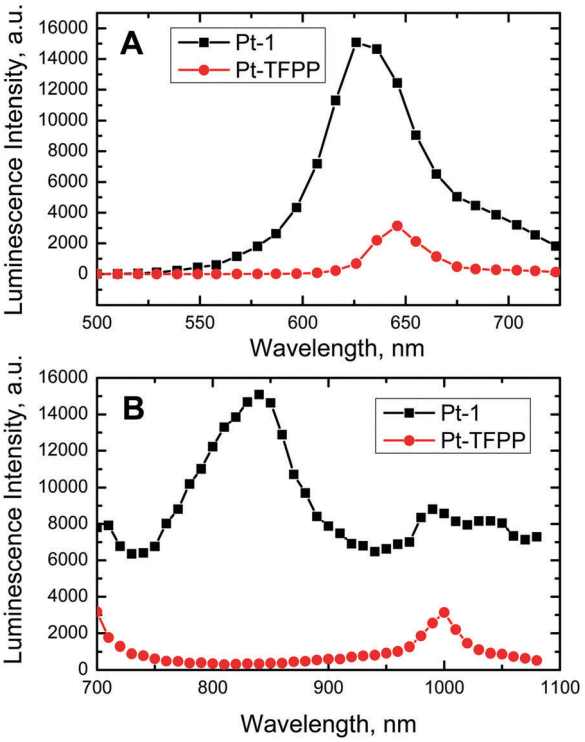

Fig. 3 Emission (A) and two photon excitation (B) spectra of Rl-100 nanoparticles stained with **Pt-1** and **Pt-TFPP**. For the emission spectra, λ_{exc} was 1050 nm and 1000 nm for **Pt-1** and **Pt-TFPP**, respectively; for the excitation spectra λ_{em} was 626 ± 5 nm and 646 ± 5 nm, respectively. The measurements were performed under anoxic conditions.

solution (~4-fold) and polystyrene (~2-fold; see below). This is likely caused by some aggregation of the very lipophilic dye in the water-swollen polar Rl-100 polymer and indicates large room for potential improvement. Increased compatibility of the dye with the polymer might be achieved *via* chemical modification of the dye with functional groups for better solubilisation or covalent immobilization. Assuming that the quantum yields under 1-P and 2-P excitation are identical, it can be concluded that the 2-P absorption cross-section of **Pt-1** is much higher (about 16-fold) compared to that of **PtTFPP**. This correlates well with the results of Xie and co-workers who determined a high 2-P absorption cross-section (190 GM) for a close analogue of **Zn-1** bearing ethyl groups instead of butyl groups.[53] It can be concluded here that the new phosphorescent emitter represents a very interesting system for potential application in 2-P microscopy due to the good match with the NIR optical window and the excellent separation of the 2-P excitation and emission peaks preventing undesired interference.

3.3 Photostability

To assess the photostability of the new Pd(II) and Pt(II) complexes, the solutions were irradiated with a high power blue LED array. The phosphorescent iridium(III) coumarin complex $Ir(C_S)_2acac$[35] was used for comparison since its photophysical properties (absorption and emission, brightness, decay time) are similar to that of Pt(II) and it proved to be a good indicator

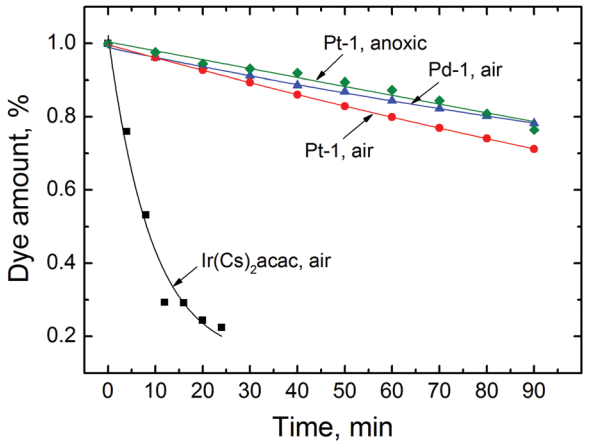

Fig. 4 Photodegradation of **Pd-1**, **Pt-1** and $Ir(C_S)_2acac$ complexes in toluene upon irradiation with a high power 458 nm 10 W LED array (photon flux 5600 μmol s^{-1} m^{-2}).

for oxygen sensing applications.[35] As can be seen (Fig. 4), the photostability of the new dyes is much better than that of the Ir(III) complex. For instance, about 3.5% of **Pt-1** is degraded upon irradiation of the air-saturated solution for 10 min. Under the same conditions, about 55% of the Ir(III) complex is destroyed. Deoxygenation of the solution of **Pt-1** improves the photostability,

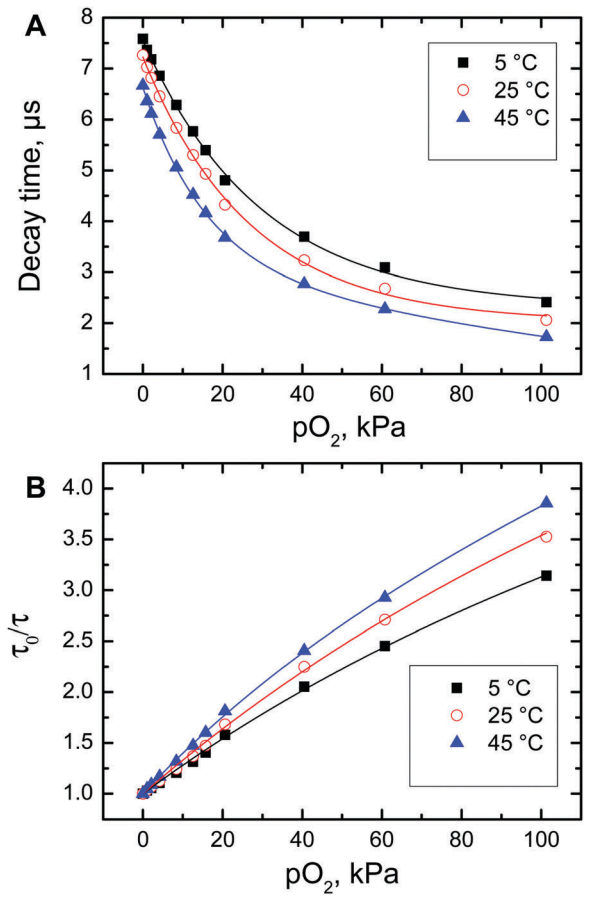

Fig. 5 Decay time (A) and Stern–Volmer (B) plots for luminescence quenching of polystyrene-immobilized **Pt-1** by oxygen.

which may indicate participation of photosensitized singlet oxygen in the photodegradation mechanism. Considering the very high intensities of the excitation light it can be concluded that the photostability of the new dyes is sufficiently good to enable virtually all potential applications.

3.4 Optical oxygen sensing

The excellent phosphorescence brightness and comparably long decay time of the **Pt-1** make it an attractive candidate for optical oxygen sensing. In order to evaluate the oxygen sensing capabilities, the dye was immobilized into polystyrene which is an attractive matrix due to high optical transparency, good mechanical properties, chemical robustness and favourable oxygen permeability. The photophysical properties of the immobilized dye (Fig. S7, ESI†) are similar to those of the solution. The absorption maxima are located at 451, 504 and 537 nm and the phosphorescence peak is at 633 nm. Upon immobilization, some decrease of the luminescence quantum yield and decay time is observed (Φ = 0.38 and τ = 7.3 μs at 25 °C and under anoxic conditions) compared to the solution, which may be due to some aggregation of the dye in the polymer since its concentration is comparably high (1 wt%).

As can be observed (Fig. 5), the oxygen sensing properties of **Pt-1** in polystyrene are similar to those of the reported phosphorescent oxygen indicators.[12] In agreement with the comparably short luminescence decay time, the dynamic range of the sensor spans from about 0.1 to 100 kPa O_2. The quenching efficiency increases with temperature. A pronounced thermal quenching of the luminescence of **Pt-1** is observed, manifested by decrease of the phosphorescence decay time in the absence of oxygen (Fig. 5A). The temperature coefficient at 25 °C is ~−0.32%τ/K. This value is significantly higher than that for Pt(II) tetraphenyltetrabenzoporphyrin (−0.06%/K)[63] but is comparable to that of the Pd(II) tetraphenyltetrabenzoporphyrin (−0.33%/K),[63] NIR-emitting Pt(II) Schiff base complexes (−0.31%/K)[41] and ruthenium(II) tris(4,7-diphenyl-1,10-phenanthroline) (−0.46%/K).[35] The results suggest that the oxygen-sensing materials based on **Pt-1** can represent an alternative to the state-of-the-art sensors. They may be particularly beneficial as 2-photon oxygen probes due to fairly strong emission under 2-P excitation and excellent compatibility with the 2-P lasers and detectors (photomultipliers) used in microscopes.

3.5 Optical temperature sensing and imaging

Oxygen-sensing experiments demonstrated significant thermal quenching of the luminescence of **Pt-1** in polystyrene. In the case of **Pd-1**, on one hand, very strong phosphorescence was observed in frozen glass in the 77 K solution, and, on the other hand, very weak emission at room temperature, suggesting even

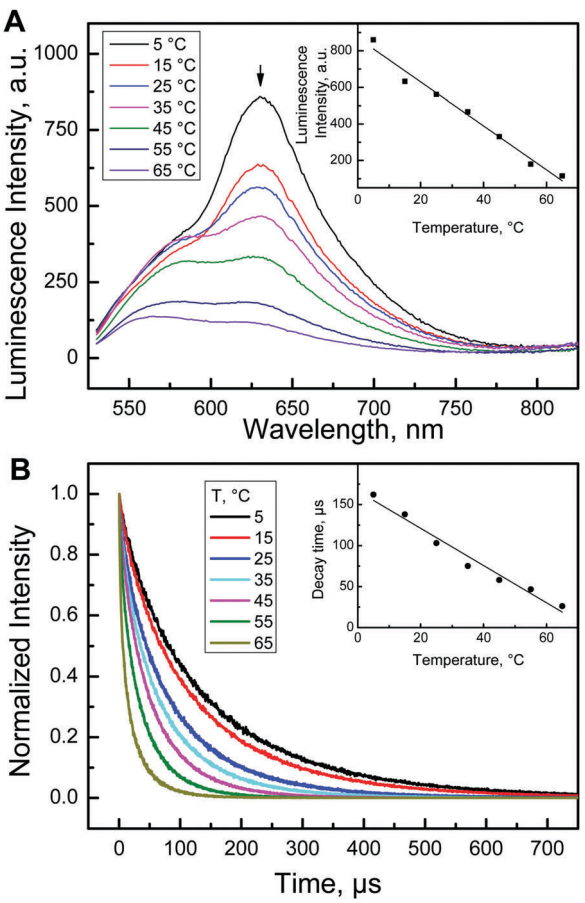

Fig. 6 Temperature-sensing properties of **Pd-1** immobilized in PViCl-PAN. (A) Temperature dependence of the emission spectra; (B) temperature dependence of the luminescence decay time.

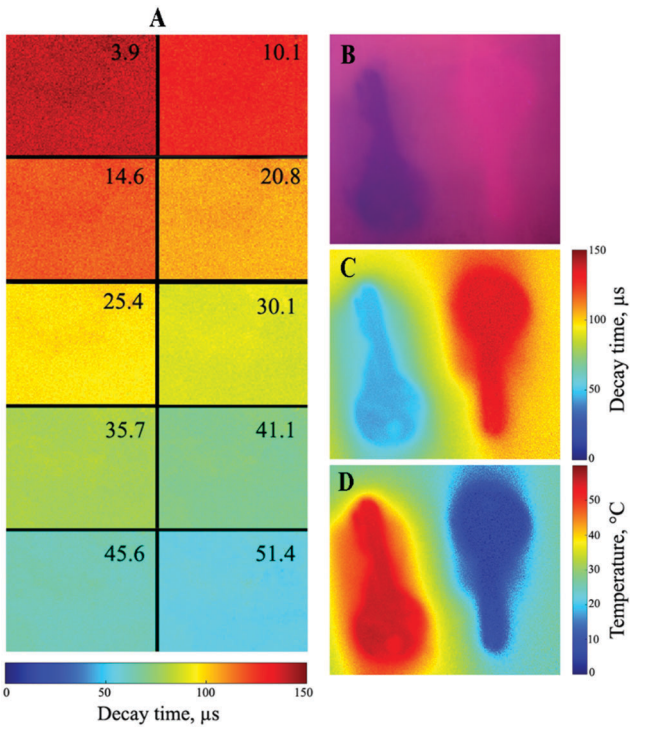

Fig. 7 Application of the **Pd-1**/PViCl-PAN planar optode for lifetime imaging of temperature. (A) False color decay time images of a sensor foil with temperatures (°C) indicated in the upper right corner. (B–D) Time-resolved imaging with the help of the same planar optode positioned over two keys. (B) RGB image of emission under excitation with a blue 465 nm LED; (C) false color decay time distribution; (D) corresponding false color image of temperature distribution.

stronger temperature effects. In order to explore the potential temperature-sensing capabilities of the new dyes, they were embedded into poly(vinylidene chloride-*co*-acrylonitrile) (PViCl-PAN) which is a polymer with extremely low oxygen permeability ($P = 0.0031 \times 10^{-13}$ cm^3(STP) cm cm^{-2} s^{-1} Pa^{-1};[64] compared to polystyrene with $P = 2 \times 10^{-13}$ cm^3(STP) cm cm^{-2} s^{-1} Pa^{-1}).[65]

Upon immobilization into the rigid polymer matrix the phosphorescence quantum yield of **Pd-1** increased to an appreciable 14% at 25 °C. Considering the high molar absorption coefficients the brightness of this material is high enough to enable sensing and imaging applications. Fig. 6A shows that the phosphorescence intensity is highly temperature-dependent. An almost linear decrease of the intensity with temperature is observed (Fig. 6A, insert). Some increase in the intensity at the shorter wavelengths may be due to appearance of the thermally-activated delayed fluorescence. Fig. 6B demonstrates that the phosphorescence decay time of **Pd-1** in PViCl-PAN also strongly decreases with temperature. Comparison of the normalized intensity and decay time dependencies (Fig. S8, ESI†) reveals the identical effect of temperature on both parameters. The temperature dependence of the luminescence decay time is of particular interest since the decay time is a self-referenced parameter which is not affected by the intensity of the excitation source, sensitivity of the photodetector, scattering and coloration of the probe *etc.* Moreover, only a few decay-time based probes (based on small molecules or inorganic phosphors) for measurements at ambient temperatures have been reported. The temperature coefficient of the decay time for the **Pd-1**/PViCl-PAN material is −2.07%/K at 25 °C and −2.76%/K at 37 °C which places the new thermometer among the most sensitive ones reported so far. For instance, the temperature coefficient at 25 °C was around −2.2%/K for Eu(III) complexes[66,67] and varied from −2.0 to −3.7%/K for the recently reported TADF emitters,[37] whereas for a ruthenium(II) tris-phenanthroline complex[68] and Cr(III)-activated yttrium aluminium borate[69] it was −0.64 and −0.9%/K, respectively. Notably, even some commercial optical thermometers utilize ruby with its moderate temperature coefficient of −0.25%/K.[70,71]

Although PViCl-PAN possesses very low oxygen permeability, some cross-talk of the temperature optode to oxygen is still possible. Indeed, at 25 °C the measured decay time changed from 103 μs in nitrogen atmosphere to 98 μs in air. This corresponds to an error of 1.2 °C if the oxygen concentration is unknown and varies over the whole range.

Imaging of the temperature distribution is another important application of molecular thermometers,[18] for instance for

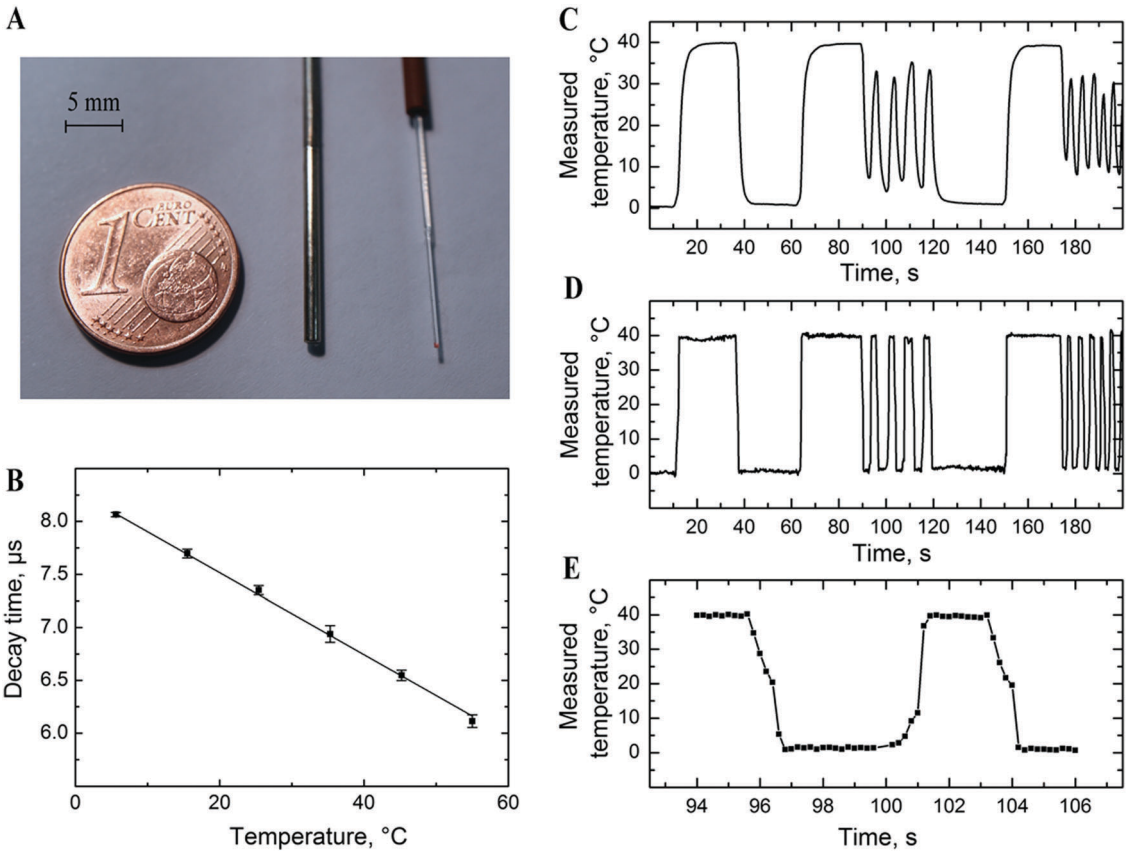

Fig. 8 Temperature-sensing properties of the **Pt-1**/PViCl-PAN microsensor. (A) Photographic image of the fiber optic microoptode (right) along with the conventional resistance thermometer PT-100 (middle) and 1 euro cent coin (left). (B) Temperature dependence of the luminescence lifetime of the sensor read-out with a Firesting compact phase fluorometer from PyroScience. (C–E) Fast temperature changes monitored by the PT 100 resistance thermometer (C) and the optical microsensor (D and E). The sensors were rapidly changed between the beakers kept at 40 °C and ~1 °C (ice water). (E) Zoom-in for the interval 94–106 s corresponding to the curve in graph D.

compensation of the temperature cross-talk of pressure-sensitive paints.[72,73] Fig. 7 demonstrates an imaging experiment performed with a gated CCD camera. The calibration plot (Fig. S9, ESI†) is similar but not fully identical to that seen in Fig. 6B. This is likely due to the fact that in the imaging experiment the so called rapid lifetime determination method[52] was used, *i.e.* the decay time is calculated from measuring the luminescence intensity in two time windows.

Fiber-optic temperature microsensors may represent a promising alternative to conventional resistance thermometers. Optical microsensors can be manufactured in different sizes which is determined by the diameter of the fiber used and whether the tip of the fiber is tapered or not. Similar to other types of luminescent microsensors, the manufacture of new temperature probes is very straightforward since the temperature-sensitive ''cocktail'' is directly coated onto the tip of the fiber (Fig. 8A). Here we use **Pt-1** embedded into PViCl-PAN although application of **Pd-1** in the same material is also possible. The behaviour of the **Pt-1**/PViCl-PAN-based material is generally similar to that of the sensor based on **Pd-1**; linear decrease of the decay time with temperature is observed (Fig. 8B). Although the temperature coefficient at 25 °C is moderate ($-0.52\%\tau$/K), it is still sufficient for reliable temperature sensing.

Due to their small size (Fig. 8A), optical temperature microsensors not only offer the advantage of measuring in small volumes but also are expected to show a fast dynamic response. The experiment shown in Fig. 8C–E confirms the above expectations. In fact, the optical microsensor excellently resolves both slow and fast temperature fluctuations (Fig. 8D). In contrast, the resistance thermometer (PT-100) followed adequately only comparably slow temperature changes but fails if the changes are too fast (Fig. 8C). The full response time of the new optical microsensor in water is less than 1 s (Fig. 8D) but is likely to be much faster since the recorded response was limited by the time necessary to transfer the sensor from one beaker into the other.

4. Conclusions

The new Schiff base metal complexes feature remarkable photophysical properties including very efficient absorption in the blue-green part of the electromagnetic spectra, room temperature phosphorescence (Pt(II) and Pd(II) complexes) or thermally-activated delayed fluorescence (Zn(II) complex) and good photostability. Moreover, the new Schiff base antenna shows efficient sensitization capabilities for generation of lanthanide luminescence. The Pt(II) complex belongs to one of the brightest phosphorescent emitters reported so far due to the combination of a high molar absorption coefficient and luminescence quantum yield. Immobilization of the Pt(II) complex into an oxygen-permeable matrix leads to a new optical oxygen sensor. Although this material is not necessarily advantageous compared to many state-of-the-art planar optodes and fiber-optic sensors, the nanoparticle-based version may be of high interest to multiphoton imaging of oxygen. Under two photon excitation, the brightness of nanobead-embedded **Pt-1** is much higher than for the Pt(II) tetra(pentafluorophenyl)-porphyrin dye. Moreover, the 2-P excitation and emission spectra of **Pt-1** show excellent compatibility with the biological optical window. Other advantages include excellent separation of the excitation and emission wavelengths and emission in the red part of the spectrum making standard photomultipliers excellently suitable for read-out.

Embedding the Pd(II) and Pt(II) dyes into a gas-blocking polymer results in powerful optical thermometers for ambient temperatures. The sensors are realized in several formats such as planar optodes and fiber-optic microsensors. These materials are essentially self-referenced since the phosphorescence decay time acts as the analytical parameter. Remarkably, the temperature coefficients for the material based on the Pd(II) complex are among the highest reported in the literature. Whereas the planar optodes are primarily intended for imaging of temperature on surfaces, the fiber-optic sensors are demonstrated to enable monitoring of very fast temperature fluctuations. In conclusion, the new group of phosphorescent emitters represents a promising platform for the design of optical sensing materials promising for a broad variety of applications.

Conflicts of interest

There are no conflicts to declare.

Acknowledgements

We thank Dr Roland Thar (PyroScience GmbH, Germany) for providing the Firesting-mini modified compact phase fluorometer and Petr Zimcik (Charles University, Hradec Kralove) for the valuable discussion. Financial Support from the ERC project ''Oxygen'' (No. 267233) and from the project EFSA-CDN (No. CZ.02.1.01/0.0/0.0/16_019/0000841) co-funded by ERDF is gratefully acknowledged.

References

1 Z. Yang, Z. Mao, Z. Xie, Y. Zhang, S. Liu, J. Zhao, J. Xu, Z. Chi and M. P. Aldred, *Chem. Soc. Rev.*, 2017, **46**, 915–1016.
2 M. Y. Wong and E. Zysman-Colman, *Adv. Mater.*, 2017, **29**, 1605444.
3 Y. Im, M. Kim, Y. J. Cho, J.-A. Seo, K. S. Yook and J. Y. Lee, *Chem. Mater.*, 2017, **29**, 1946–1963.
4 Y. Tao, K. Yuan, T. Chen, P. Xu, H. Li, R. Chen, C. Zheng, L. Zhang and W. Huang, *Adv. Mater.*, 2014, **26**, 7931–7958.
5 H. Xiang, J. Cheng, X. Ma, X. Zhou and J. J. Chruma, *Chem. Soc. Rev.*, 2013, **42**, 6128–6185.
6 R. C. Evans, P. Douglas and C. J. Winscom, *Coord. Chem. Rev.*, 2006, **250**, 2093–2126.
7 J. Kalinowski, V. Fattori, M. Cocchi and J. A. G. Williams, *Coord. Chem. Rev.*, 2011, **255**, 2401–2425.
8 S. Hirata, K. Totani, J. Zhang, T. Yamashita, H. Kaji, S. R. Marder, T. Watanabe and C. Adachi, *Adv. Funct. Mater.*, 2013, **23**, 3386–3397.

9 X. Lixin, C. Zhijian, Q. Bo, L. Jiaxiu, K. Sheng, G. Qihuang and K. Junji, *Adv. Mater.*, 2011, **23**, 926–952.
10 C. Bizzarri, F. Hundemer, J. Busch and S. Bräse, *Polyhedron*, 2018, **140**, 51–66.
11 H. Uoyama, K. Goushi, K. Shizu, H. Nomura and C. Adachi, *Nature*, 2012, **492**, 234–238.
12 M. Quaranta, S. M. Borisov and I. Klimant, *Bioanal. Rev.*, 2012, **4**, 115–157.
13 Q. Zhao, F. Li and C. Huang, *Chem. Soc. Rev.*, 2010, **39**, 3007–3030.
14 X. Wang and O. S. Wolfbeis, *Chem. Soc. Rev.*, 2014, **43**, 3666–3761.
15 D. B. Papkovsky and R. I. Dmitriev, *Chem. Soc. Rev.*, 2013, **42**, 8700–8732.
16 B. Nacht, C. Larndorfer, S. Sax, S. M. Borisov, M. Hajnsek, F. Sinner, E. J. W. List-Kratochvil and I. Klimant, *Biosens. Bioelectron.*, 2015, **64**, 102–110.
17 L. Tormo, N. Bustamante, G. Colmenarejo and G. Orellana, *Anal. Chem.*, 2010, **82**, 5195–5204.
18 X. Wang, O. S. Wolfbeis and R. J. Meier, *Chem. Soc. Rev.*, 2013, **42**, 7834–7869.
19 D. B. Papkovsky and T. C. O'Riordan, *J. Fluoresc.*, 2005, **15**, 569–584.
20 Q. Zhao, C. Huang and F. Li, *Chem. Soc. Rev.*, 2011, **40**, 2508–2524.
21 Y. You, *Curr. Opin. Chem. Biol.*, 2013, **17**, 699–707.
22 T. N. Singh-Rachford and F. N. Castellano, *Coord. Chem. Rev.*, 2010, **254**, 2560–2573.
23 J. Zhao, S. Ji and H. Guo, *RSC Adv.*, 2011, **1**, 937–950.
24 J. Zhou, Q. Liu, W. Feng, Y. Sun and F. Li, *Chem. Rev.*, 2015, **115**, 395–465.
25 S. Mukherjee and P. Thilagar, *Chem. Commun.*, 2015, **51**, 10988–11003.
26 G. He, B. D. Wiltshire, P. Choi, A. Savin, S. Sun, A. Mohammadpour, M. J. Ferguson, R. McDonald, S. Farsinezhad, A. Brown, K. Shankar and E. Rivard, *Chem. Commun.*, 2014, **51**, 5444–5447.
27 M. S. Kwon, D. Lee, S. Seo, J. Jung and J. Kim, *Angew. Chem., Int. Ed.*, 2014, **126**, 11359–11363.
28 Y. Gong, G. Chen, Q. Peng, W. Z. Yuan, Y. Xie, S. Li, Y. Zhang and B. Z. Tang, *Adv. Mater.*, 2015, **27**, 6195–6201.
29 Z. An, C. Zheng, Y. Tao, R. Chen, H. Shi, T. Chen, Z. Wang, H. Li, R. Deng, X. Liu and W. Huang, *Nat. Mater.*, 2015, **14**, 685–690.
30 C. Zhou, T. Xie, R. Zhou, C. O. Trindle, Y. Tikman, X. Zhang and G. Zhang, *ACS Appl. Mater. Interfaces*, 2015, **7**, 17209–17216.
31 G. Khalil, M. Gouterman, S. Ching, C. Costin, L. Coyle, S. Gouin, E. Green, M. Sadilek, R. Wan, J. Yearyean and B. Zelelow, *J. Porphyrins Phthalocyanines*, 2002, **6**, 135–145.
32 D. B. Papkovsky, G. V. Ponomarev, W. Trettnak and P. O'Leary, *Anal. Chem.*, 1995, **67**, 4112–4117.
33 P. C. Alford, M. J. Cook, A. P. Lewis, G. S. G. McAuliffe, V. Skarda, A. J. Thomson, J. L. Glasper and D. J. Robbins, *J. Chem. Soc., Perkin Trans. 2*, 1985, 705–709.
34 Y. Chi and P.-T. Chou, *Chem. Soc. Rev.*, 2010, **39**, 638–655.
35 S. M. Borisov and I. Klimant, *Anal. Chem.*, 2007, **79**, 7501–7509.
36 P. Duan, N. Yanai and N. Kimizuka, *Chem. Commun.*, 2014, **50**, 13111–13113.
37 A. Steinegger, I. Klimant and S. M. Borisov, *Adv. Opt. Mater.*, 2017, **5**, 1700372.
38 C.-M. Che, S.-C. Chan, H.-F. Xiang, M. C. W. Chan, Y. Liu and Y. Wang, *Chem. Commun.*, 2004, 1484.
39 C.-M. Che, C.-C. Kwok, S.-W. Lai, A. F. Rausch, W. J. Finkenzeller, N. Zhu and H. Yersin, *Chem. – Eur. J.*, 2010, **16**, 233–247.
40 J. Zhang, F. Zhao, X. Zhu, W.-K. Wong, D. Ma and W.-Y. Wong, *J. Mater. Chem.*, 2012, **22**, 16448–16457.
41 S. M. Borisov, R. Saf, R. Fischer and I. Klimant, *Inorg. Chem.*, 2013, **52**, 1206–1216.
42 J. Zhang, G. Dai, F. Wu, D. Li, D. Gao, H. Jin, S. Chen, X. Zhu, C. Huang and D. Han, *J. Photochem. Photobiol., A*, 2016, **316**, 12–18.
43 A. Monguzzi, S. M. Borisov, J. Pedrini, I. Klimant, M. Salvalaggio, P. Biagini, F. Melchiorre, C. Lelii and F. Meinardi, *Adv. Funct. Mater.*, 2015, **25**, 5617–5624.
44 J. Zhang, L. Xu and W.-Y. Wong, *Coord. Chem. Rev.*, 2018, **355**, 180–198.
45 M. Dramicanin, *Luminescence Thermometry, Methods, Materials, and Applications*, Elsevier, Woodhead Publishing, 1st edn, 2018.
46 W. J. Youngblood, *J. Org. Chem.*, 2006, **71**, 3345–3356.
47 P. Zimcik, M. Miletin, H. Radilova, V. Novakova, K. Kopecky, J. Svec and E. Rudolf, *Photochem. Photobiol.*, 2010, **86**, 168–175.
48 A. Fercher, S. M. Borisov, A. V. Zhdanov, I. Klimant and D. B. Papkovsky, *ACS Nano*, 2011, **5**, 5499–5508.
49 G. A. Crosby and J. N. Demas, *J. Phys. Chem.*, 1971, **75**, 991–1024.
50 G. Seybold and G. Wagenblast, *Dyes Pigm.*, 1989, **11**, 303–317.
51 A. K. Bansal, W. Holzer, A. Penzkofer and T. Tsuboi, *Chem. Phys.*, 2006, **330**, 118–129.
52 G. Liebsch, I. Klimant, B. Frank, G. Holst and O. Wolfbeis, *Appl. Spectrosc.*, 2000, **54**, 548–559.
53 D. Xie, J. Jing, Y.-B. Cai, J. Tang, J.-J. Chen and J.-L. Zhang, *Chem. Sci.*, 2014, **5**, 2318–2327.
54 J. Zhao, F. Dang, B. Liu, Y. Wu, X. Yang, G. Zhou, Z. Wu and W.-Y. Wong, *Dalton Trans.*, 2017, **46**, 6098–6110.
55 J. Zhao, B. Liu, Z. Feng, D. Jin, W. Dang, X. Yang, G. Zhou, Z. Wu and W.-Y. Wong, *Polym. Chem.*, 2017, **8**, 6368–6377.
56 X. Zhu, W.-K. Wong, W.-Y. Wong and X. Yang, *Eur. J. Inorg. Chem.*, 2011, 4651–4674.
57 X. Yang, R. A. Jones and W.-K. Wong, *Dalton Trans.*, 2008, 1676–1678.
58 G. S. He, L.-S. Tan, Q. Zheng and P. N. Prasad, *Chem. Rev.*, 2008, **108**, 1245–1330.
59 Y. Chen, R. Guan, C. Zhang, J. Huang, L. Ji and H. Chao, *Coord. Chem. Rev.*, 2016, **310**, 16–40.
60 T. V. Esipova and S. A. Vinogradov, *J. Org. Chem.*, 2014, **79**, 8812–8825.

61 E. Roussakis, J. A. Spencer, C. P. Lin and S. A. Vinogradov, *Anal. Chem.*, 2014, **86**, 5937–5945.
62 T. V. Esipova, H. J. Rivera-Jacquez, B. Weber, A. E. Masunov and S. A. Vinogradov, *J. Phys. Chem. A*, 2017, **121**, 6243–6255.
63 S. M. Borisov, G. Nuss and I. Klimant, *Anal. Chem.*, 2008, **80**, 9435–9442.
64 R. A. Wessling, D. S. Gibbs, B. E. Obi, D. E. Beyer, P. T. DeLassus and B. A. Howell, *Encyclopedia of Polymer Science and Technology*, John Wiley & Sons, Inc, Hoboken, 2002, pp. 458–510.
65 J. Brandrup, E. H. Immergut and E. A. Grulke, *Polymer Handbook*, John Wiley & Sons Inc, New York, 1999.
66 G. E. Khalil, K. Lau, G. D. Phelan, B. Carlson, M. Gouterman, J. B. Callis and L. R. Dalton, *Rev. Sci. Instrum.*, 2004, **75**, 192.
67 H. Peng, M. I. J. Stich, J. Yu, L. Sun, L. H. Fischer and O. S. Wolfbeis, *Adv. Mater.*, 2010, **22**, 716–719.
68 G. Liebsch, I. Klimant and O. S. Wolfbeis, *Adv. Mater.*, 1999, **11**, 1296–1299.
69 S. M. Bori‘sov, K. Gatterer, B. Bitschnau and I. Klimant, *J. Phys. Chem. C*, 2010, **114**, 9118–9124.
70 H. Aizawa, N. Ohishi, S. Ogawa, T. Katsumata, S. Komuro, T. Morikawa and E. Toba, *Rev. Sci. Instrum.*, 2002, **73**, 3656–3658.
71 Y. L. Hu, Z. Y. Zhang, K. T. V. Grattan, A. W. Palmer and B. T. Meggitt, *Sens. Actuators, A*, 1997, **63**, 85–90.
72 J. Hradil, C. Davis, K. Mongey, C. McDonagh and B. D. MacCraith, *Meas. Sci. Technol.*, 2002, **13**, 1552–1557.
73 M. E. Köse, B. F. Carroll and K. S. Schanze, *Langmuir*, 2005, **21**, 9121–9129.